ARTICLE
Journal of Cellular Biochemistry 109:58–64 (2010)

Journal of Cellular Biochemistry

Real-Time Imaging of Single Cancer-Cell Dynamics of Lung Metastasis

Hiroaki Kimura,[1,2,3] Katsuhiro Hayashi,[3] Kensuke Yamauchi,[3] Norio Yamamoto,[3] Hiroyuki Tsuchiya,[3] Katsuro Tomita,[3] Hiroyuki Kishimoto,[1] Michael Bouvet,[2] and Robert M. Hoffman[1,2*]

[1]*AntiCancer, Inc., 7917 Ostrow Street, San Diego, California 92111*

[2]*Department of Surgery, University of California, San Diego, 200 West Arbor Drive, San Diego, California 92103-8220*

[3]*Department of Orthopaedic Surgery, Graduate School of Medical Science, Kanazawa University, Kanazawa, Ishikawa, Japan*

ABSTRACT

We have developed a new in vivo mouse model to image single cancer-cell dynamics of metastasis to the lung in real-time. Regulating airflow volume with a novel endotracheal intubation method enabled controlling lung expansion adequate for imaging of the exposed lung surface. Cancer cells expressing green fluorescent protein (GFP) in the nucleus and red fluorescent protein (RFP) in the cytoplasm were injected in the tail vein of the mouse. The right chest wall was then opened in order to image metastases on the lung surface directly. After each observation, the chest wall was sutured and the air was suctioned in order to re-inflate the lung, in order to keep the mice alive. Observations have been carried out for up to 8 h per session and repeated up to six times per mouse thus far. The seeding and arresting of single cancer cells on the lung, accumulation of cancer-cell emboli, cancer-cell viability, and metastatic colony formation were imaged in real-time. This new technology makes it possible to observe real-time monitoring of cancer-cell dynamics of metastasis in the lung and to identify potential metastatic stem cells. J. Cell. Biochem. 109: 58–64, 2010.

KEY WORDS: FLUORESCENT PROTEINS; REAL-TIME IMAGING; LUNG METASTASIS; CELLULAR DYNAMICS

The lung is often the site of cancer metastases which are usually highly treatment resistant. However, the process through which circulating tumor cells form lung metastatic colonies is still poorly understood, because the lung is the most challenging organ to observe in mouse models. The anatomical position of the lung precludes noninvasive single-cell imaging. Respiratory and cardiac movements prevent accurate imaging. Most critically, once the chest wall is opened, the mouse dies within 5 min due to pneumothorax. Therefore, current methods to observe lung metastasis in mice are ex vivo [Yamamoto et al., 2003a].

Our laboratory pioneered in vivo imaging with green fluorescent protein (GFP) and/or red fluorescent protein (RFP). These very bright proteins have made it possible to observe cellular behavior in primary tumors and metastases in live animals [Chishima et al., 1997; Yang et al., 2000; Hoffman, 2005]. With the use of fluorescent proteins and a sensitive imaging system, Yamamoto et al. reported that lung metastases derived from human fibrosarcoma cells tagged with GFP could be visualized through the intact chest wall after opening a skin-flap window [Yamamoto et al., 2003b]. The technique enabled real-time imaging of the lung metastases in the same mouse at the colony level.

Dual-color cancer cells, in which GFP is expressed in the nucleus and RFP is expressed in the cytoplasm, were developed in our laboratory [Yamamoto et al., 2004] to enable real-time nuclear-cytoplasmic dynamics to be visualized in living cells in vivo [Yamauchi et al., 2005, 2006].

In this report, we have developed a new in vivo mouse model to observe lung metastasis longitudinally at the cellular and subcellular level with dual-color cancer cells. We were able to observe single cancer cells seeding the lungs of live mice in real-time and follow them in the same mouse using a novel endotracheal intubation method to keep the mice alive for 8 h per imaging session with the lungs exposed along with a variable magnification mouse

Additional Supporting Information may be found in the online version of this article.

Grant sponsor: National Cancer Institute; Grant number: CA132971.

*Correspondence to: Robert M. Hoffman, PhD, AntiCancer Inc., 7917 Ostrow Street, San Diego, CA 92111.
E-mail: all@anticancer.com

Received 11 September 2009; Accepted 15 September 2009 • DOI 10.1002/jcb.22379 • © 2009 Wiley-Liss, Inc.
Published online 12 November 2009 in Wiley InterScience (www.interscience.wiley.com).

imaging system to detect single cells in vivo. This new technology will enable the in vivo cell biology of the initial and subsequent steps of metastasis to be much better understood.

MATERIALS AND METHODS

ESTABLISHMENT OF DUAL-COLOR CANCER CELL LINES

To establish MMT-060562 murine mammary carcinoma (MMT) or HT1080 human fibrosarcoma (HT1080) GFP-RFP cells, the cells were transfected with retroviral DsRed2 and H2B-GFP vectors as previously described [Yamamoto et al., 2004]. In brief, the *Hin*d III/*Not* I fragment from pDsRed2 (Clontech Laboratories, Inc., Palo Alto, CA), containing the full-length RFP cDNA, was inserted into the *Hin*d III/*Not* I site of pLNCX2 (Clontech Laboratories, Inc.) containing the neomycin resistance gene. PT67, a NIH3T3-derived packaging cell line (Clontech Laboratories, Inc.) expressing the 10 Al viral envelope, was cultured in DMEM (Irvine Scientific, Santa Ana, CA) supplemented with 10% heat-inactivated fetal bovine serum (FBS; Gemini Bio-Products). For vector production, PT67 cells, at 70% confluence, were incubated with a precipitated mixture of LipofectAMINE reagent (Life Technologies, Inc., Grand Island, NY) and saturating amounts of pLNCX2-DsRed2 plasmid for 18 h. Fresh medium was replenished at this time. The cells were examined by fluorescence microscopy 48 h post-transfection. For selection of a clone producing high amounts of a RFP retroviral vector (PT67-DsRed2), the cells were cultured in the presence of 200–800 μg/ml G418 (Life Technologies, Inc.) increased stepwise over 7 days.

The histone H2B gene has no stop codon, thereby enabling the ligation of the H2B gene to the 5′-coding region of the GFP gene (Clontech Laboratories, Inc.). The histone H2B-GFP fusion gene was then inserted at the *Hin*d III/*Cal* I site of the pLHCX (Clontech Laboratories, Inc.) that has the hygromycin resistance gene. To establish a packaging cell clone producing high amounts of histone H2B-GFP retroviral vector, the pLHCX histone H2B-GFP plasmid was transfected in PT67 cells using the same methods described above for PT67-DsRed2. The transfected cells were cultured in the presence of 200–800 μg/ml hygromycin (Life Technologies, Inc.) increased stepwise over 7 days.

For RFP and H2B-GFP gene transduction, 70% confluent MMT or HT1080 cells were used. To establish dual-color cells, clones of these cells expressing RFP in the cytoplasm were initially established. In brief, cells were incubated with a 1:1 precipitated mixture of retroviral supernatants of PT67-RFP cells and RPMI 1640 (Irvine Scientific) containing 10% FBS for 72 h. Fresh medium was replenished at this time. Cells were harvested with trypsin/EDTA 72 h post-transduction and subcultured at a ratio of 1:15 into selective medium, which contained 200 μg/ml G418. The level of G418 was increased stepwise up to 800 μg/ml.

For establishing dual-color cells, cells were then incubated with a 1:1 precipitated mixture of retroviral supernatants of PT67 H2B-GFP cells and culture medium. To select the double transformants, cells were incubated with hygromycin 72 h after transfection. The level of hygromycin was increased stepwise from 200 to 800 μg/ml (Fig 1a, 1b).

PROLIFERATION OF FLUORESCENT PROTEIN-LABELED CELLS IN VITRO

Dual-color HT1080 or MMT cells were seeded at a density of 1×10^3 cells/dish in 100-mm dishes with RPMI with 10% FBS medium (day 1). The dishes were kept in an incubator at 37°C and 5% CO_2. Every other day (days 2–8), three dishes for each clone were used for cell counting. In brief, resuspended cells collected after trypsinization were stained with trypan blue (Sigma-Aldrich, St. Louis, MO). Only viable cells were counted with a hemocytometer (Hausser Scientific, Horsham, PA).

MICE

Athymic NCR nude mice (*nu*/*nu*) and C57BL/6 mice, at 4–6 weeks of age, were used in this study. The breeding pairs were obtained from Charles River Laboratories. Mice were kept in a barrier facility under HEPA filtration. Mice were fed with autoclaved laboratory rodent diet. All animal studies were conducted in accordance with the principals and procedures outlined in the NIH Guide for the Care and Use of Laboratory Animals under assurance number A3873-1.

DEVELOPMENT OF A NOVEL MOUSE ENDOTRACHEAL INTUBATION PROCEDURE

We developed a novel retrograde wire-guided endotracheal intubation procedure for mice. The mice were anesthetized with a ketamine mixture (10 μl ketamine HCL, 7.6 μl xylazine, 2.4 μl acepromazine maleate, and 10 μl H_2O s.c.) via s.c. injection. The mice were then placed supine on a glass Thermo Plate (Olympus Corp., Tokyo, Japan) in order to maintain constant body temperature throughout the experiment and fixed with plastic tape. A cylindrical column, for example, a lid of needle, was put under the neck to extend the head and neck. An intravenous catheter (SURFLO®, 20 gauge, 25 mm length; Terumo Medical Corporation, Elkton, MD) was used as an endotracheal tube. The catheter had a round molded tip to prevent damage to the soft tissue by sharp edges. This was achieved by briefly placing the tip in an open flame. A 5 mm skin incision was made above the trachea, and then the subcutaneous tissue was separated and the submandibular gland was moved aside to expose the trachea. This made it facile to confirm if intubation was successful and not into the esophagous (Supplemental Fig. 1b). A small hole (about 1 mm in diameter) was then made on the trachea with a 27-gauge needle (Becton Dickinson & Co., Franklin Lakes, NJ) in order to insert a guide wire (monofilament wire, 0.28 mm in diameter) which was inserted through the mouth (Supplemental Fig. 1c). The endotracheal catheter could then be accurately introduced into the trachea over the guide wire (Supplemental Fig. 1d). An adequate intubation depth was obtained when the root of the catheter reached the incisors.

After endotracheal intubation, the intubation tube was attached and tied to a Y-type connector (3.2 mm OD, Nalgene, Rochester, NY), and a 5-cm exhaust tubing (1.47 mm ID, 1.96 mm OD) was attached to one end of the Y-shape connector. The oxygen tube was connected to the Y-shaped connector. At this point, the chest cavity was opened. To maintain anesthesia throughout the procedure, an inhalant anesthesia system, Portable Anesthesia Machine (PAM, Summit Anesthesia Solutions, Bend, OR, Part Number AS-01-0007) and a precision Tec 3 Isoflurane vaporizer pin (Summit Anesthesia

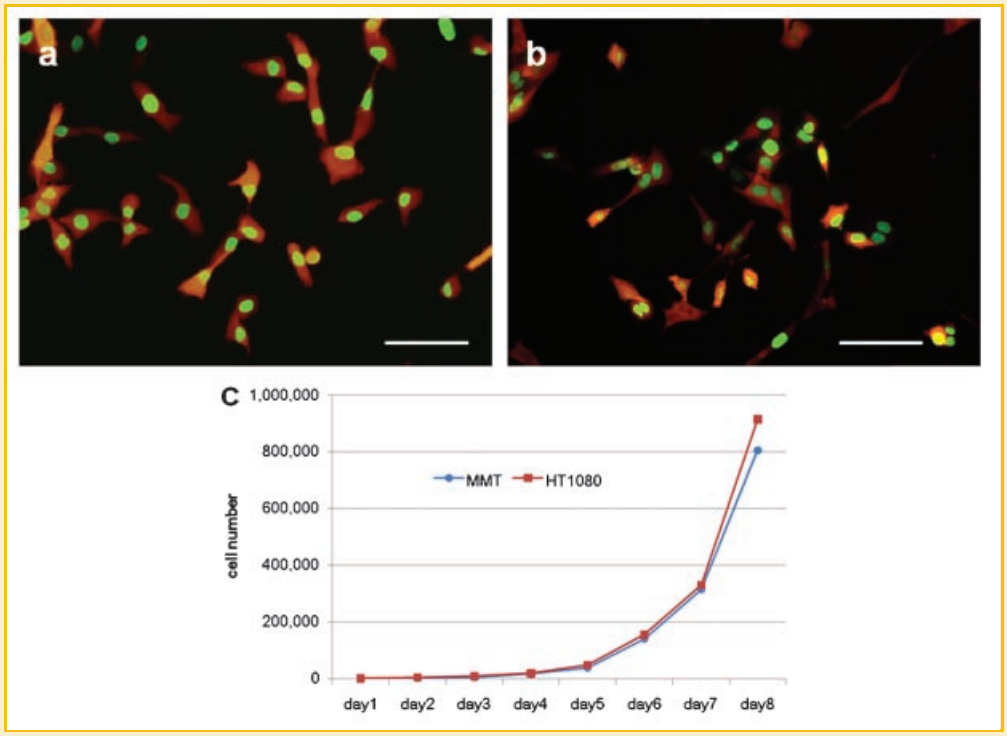

Fig. 1. GFP-RFP-expressing cancer cells. a,b: Stable high GFP- and RFP-expressing HT1080 and MMT cells in vitro, respectively. Cells were initially transduced with RFP and the neomycin resistance gene. The cells were subsequently transduced with histone H2B-GFP and the hygromycin resistance gene on a retrovirus vector. Double transformants were selected with G418 and hygromycin, and stable clones were established. Scale bar, 100 μm. HT1080 cells were larger than MMT cells. c: Cell proliferation potential of dual-color HT1080 and MMT cells. Three dishes of each cell line were used at each time point for cell counting. Cells were trypsinized, stained with trypan blue, and counted in a hemocytometer. The average number of cells for each group was calculated. There was no significant difference in the proliferation rates between HT1080 cells.

Solutions, Part Number AA-00-1041-P) were used. The carrier gas was 100% oxygen supplied in E-tanks. The oxygen flow rate was set at 100 cc/min. The vaporizer was set at 1.0 % isoflurane (Isothesia, Butler Animal Health Supply, Dublin, OH) per volume of oxygen (Fig. 2a).

REGULATION OF VENTILATION FOR OPEN CHEST IMAGING

To open the chest cavity, a 1-cm skin incision was made on the right side of the chest. The chest wall was opened without any injury to the lung. Then, an exhaust tube was half clamped to inflate the lung. This Positive End Expiratory Pressure (PEEP) system made it possible not only to keep the animal alive but also to regulate lung inflation and deflation. By adjusting the PEEP to the proper pressure, the lungs were inflated to the proper fullness to optimally image cancer cells seeding the lung (Fig. 2b). The mouse was ventilated at proper frequency by closing and opening the exhaust tube. After each observation period, the chest wall was closed with 6-0 sutures. During suturing, slight pressure was applied on the chest in order to reduce the volume of air in the chest cavity. The remaining air inside of the chest cavity was then suctioned in order to re-inflate the lung. The intubation tube was extubated when the mouse was breathing sufficiently. The mouse could be kept alive, and we could observe the same developing metastatic colony at any time by reopening the chest wall with the techniques described above. Observations have been carried out for up to 8 h and repeated up to six times per mouse thus far.

IMAGING SINGLE CANCER CELL SEEDING ON THE LUNG

The intubated mouse was placed in an OV100 Small Animal Imaging System (Olympus Corp., Tokyo, Japan) to observe cancer cell dynamics of lung seeding after tail-vein injection. Dual-color HT1080 or MMT cells were injected via tail vein and imaging was immediately started. Real-time movies of cancer cell seeding were produced. High-resolution images were captured directly on a PC (Fujitsu Siemens, Munich, Germany).

TIME COURSE OF CANCER CELL SURVIVAL AFTER SEEDING THE LUNG

A total of 200 μl medium containing 2×10^5 dual-color HT1080 or MMT cells were injected into the tail vein of nude mice to compare the seeding capability of these cells. The lung was exposed by the technique described above and two fields of the lung were imaged (1.65 mm × 2.15 mm) in each mouse at 6 h (day 0), 1 day and 7 days after cancer cell injection. The total number of tumor cells or cell aggregates or colonies on the lung surface was counted using Scion Image (Scion; www.scioncorp.com). Five mice were used for each group. The experimental data were expressed as the mean × SE of five mice. Statistical differences between HT1080 and MMT were analyzed using the Student's *t*-test.

TIME COURSE OF METASTATIC COLONY FORMATION AND COLONY PROLIFERATION RATES IN THE LUNG

Based on the time course of cancer cell survival after seeding in the lung, a total of 200 μl medium containing 2×10^5 dual-color MMT

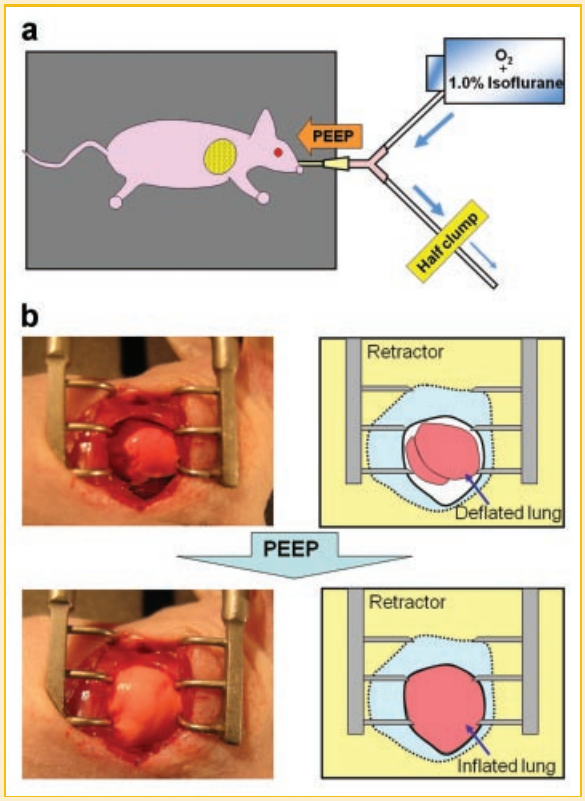

Fig. 2. Ventilation system for lung imaging. a: An intubation tube was tied to Y-type connector and an exhaust tubing was attached to one of the ends. The oxygen tube was connected to a Y-shape connector. The chest cavity was then opened. To maintain anesthesia throughout the procedure, an inhalant anesthesia system was used. The oxygen flow rate was set at 100 cc/min. The vaporizer was set at 1.0 % isoflurane per volume of oxygen. In order to control inflation of the lung, the exhaust tube was half clamped. b: After opening the chest wall, the lung was immediately deflated. Adjusting the PEEP system allowed the lung to inflate to the proper fullness.

cells were injected into the tail vein of nude mice. The lung was imaged six times, once every 3 days (from day 1 to day 16) by the techniques described above. The same metastatic colonies were measured over this time period.

RESULTS

CELL PROLIFERATION RATES OF HT1080 AND MMT DUAL-COLOR CELLS IN VITRO

The selected dual-color HT1080 and MMT cells have bright GFP and RFP fluorescence in vitro (Fig. 1a,b). All cells in the population express both GFP and RFP, indicating stability of both transgenes. HT1080 dual-color cells were larger than MMT dual-color cells. There was no significant difference in the proliferation rates of HT1080 dual-color, or MMT dual-color clones determined in monolayer culture (Fig. 1c).

EVALUATION OF A NOVEL MOUSE ENDOTRACHAEL INTUBATION PROCEDURE

To determine the toxicity of retrograde wire-guided endotracheal intubation, 10 athymic NCR nude mice and 10 C57BL/6 mice were used to compare the difference between strains. This intubation was repeated 1 week after the initial intubation in order to verify if it would be possible to re-intubate in the mice. Ten non-intubated and only anesthetized mice served as controls for possible toxicity of this method. Body weight was measured each day for 2 weeks. Retrograde guide wire insertion enabled the intubation tube to enter the trachea accurately and easily. The success rate of initial intubation was 100%. The mean time of initial intubation was 129.5 s (88–176 s). Upon repeated intubation 1 week after the initial intubation, there was no additional difficulty and the success rate of repeated intubation was also 100%. No major complications occurred. In one case, a hole on the trachea widened during retrograde guide wire insertion. A single suture narrowed the hole. No air-leakage or difficulty of repeated intubation occurred. In the other mice, the small hole did not widen. Air-leakage, after removal of the intubation tube and skin suture, did not occur. Weekly intubation had no effect on body weight compared with the control group. No blood was observed on the intubation tube. No bleeding was observed after intubation. None of the animals had physical or behavioral evidence of injury or bleeding the following day.

REAL-TIME IMAGING OF HT1080 OR MMT CELL SEEDING ON THE LUNG

To visualize cancer-cell dynamics during lung metastasis in live mice, a total of 200 μl medium containing 1×10^6 dual-color HT1080 cells or dual-color MMT cells were injected into the tail vein of nude mice. Real-time movies of cancer cell seeding were produced (Supplemental Movie 1). Approximately 5 s after cell injection, cancer cells reached the lung and formed emboli. This real-time imaging indicated that a single cancer cell was first in the capillary and then additional cancer cells also arrested in the same location and formed emboli. Macro images showed that cancer cells were distributed homogeneously in the blood vessels on the lung surface (Supplementary Fig. 2).

TIME COURSE OF CANCER CELL SURVIVAL AFTER SEEDING THE LUNG

In the lung, a large number of injected cancer cells were arrested at day 0. The number of HT1080 cells that arrested were significantly larger than that of MMT despite the same number of cells that were injected (Fig. 3a,d,g). This difference seemed to be caused by the size of each cell, namely the HT1080 cell was larger than the MMT cell (Fig. 1a,b). The smaller a cancer cell is, the easier it can pass through capillaries.

The number of HT1080 cells arrested in the lung at day 1 decreased rapidly to less than 20% of the number of arrested cells on day 0. In contrast, more than 50% of the MMT cells arrested on day 0 remained on day 1 (Fig. 3b,e,g). Interestingly, mostly single cells or groups of two cells were observed to be arrested on day 1 even though they formed emboli on day 0. This finding suggested that among the cells which formed emboli, only a few cells could sufficiently attach to the vessel wall and remain in the lung. It is also possible that most of the cancer cells arrested in the original emboli could not survive. The remaining cells would then form colonies.

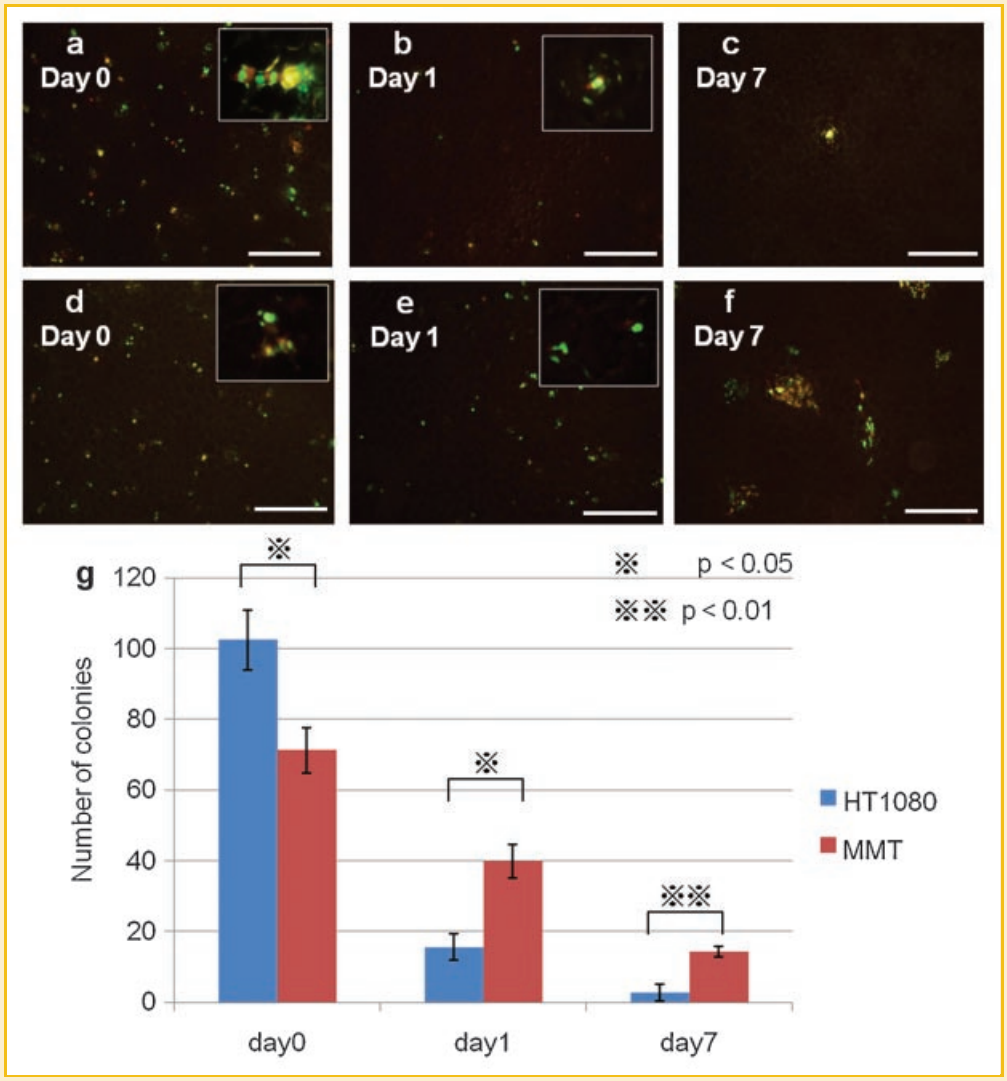

Fig. 3. Imaging survival of lung-seeded cancer cells. 2×10^5 dual-color HT1080 or MMT cells were injected in the tail vein of nude mice to compare their seeding capability. The lung was exposed and two fields (1.65 mm × 2.15 mm) were imaged in each mouse at 6 h (day 0), 1 day and 7 days after injection. a–c: Time course imaging of lung after dual-color HT1080 cell injection. Scale bar, 500 μm. Cancer cells gradually disappeared overtime. At day 7, only one colony would be observed. Most arrested cancer cells were single cells or two cells at day 1 even though they formed emboli at day 0. d–f: Time-course imaging of the lung after dual-color MMT cell injection. Scale bar, 500 μm. MMT cells arrested and colonized at a greater frequency than HT1080 cells. g: The total number of cancer cell or cell aggregates or colonies on the lung surface at each day was counted. Five mice were used for each group. The experimental data were expressed as the mean ± SE. The statistical difference between HT1080 and MMT was analyzed by the Student's *t*-test. At day 0, the number of HT1080 cell aggregates was significantly larger than that of MMT. At day 1 and day 7, however, the number of HT1080 aggregates was significantly smaller than that of MMT.

By day 7, an average of over 10 colonies of MMT GFP-RFP per field was observed. In contrast, only a few colonies of HT1080 were observed (Fig. 3c,f,g).

REAL-TIME IMAGING OF LUNG METASTATIC COLONY FORMATION

We visualized lung metastatic colonies in live mice 10 days after 1×10^6 dual-color HT1080 or 2×10^5 dual-color MMT cells were injected. Lung metastatic colonies were visualized from the macro to the subcellular level. Supplemental movie 2 shows tumor colony formation. These colonies were not visible with brightfield illumination. The metastatic colonies were mostly round or oval at the macro level. However, there was a morphological difference between the HT1080 colonies and those of MMT at the micro level. The margin of the HT1080 colonies was distinct and each cell in the colony appeared rounded (Fig. 4a–d), whereas the margin of the MMT colonies was unclear and the cytoplasm of MMT cells was stretched and infiltrated outside of the colony margin (Fig. 4e–h).

By enabling the mice to survive with our procedure, we could carry out time-course imaging of lung metastatic colony progression in live mice. A total of 200 μl medium containing 2×10^5 dual-color MMT cells were injected into the tail vein of nude mice. Four colonies that still survived at final observation were able to be observed six times, once every 3 days, from day 1 to day 16 at the same magnification. Fig. 5a–f shows time-course growth of the same colonies. Most colonies continued to increase in size, while a few colonies disappeared spontaneously. In the first week, their growth

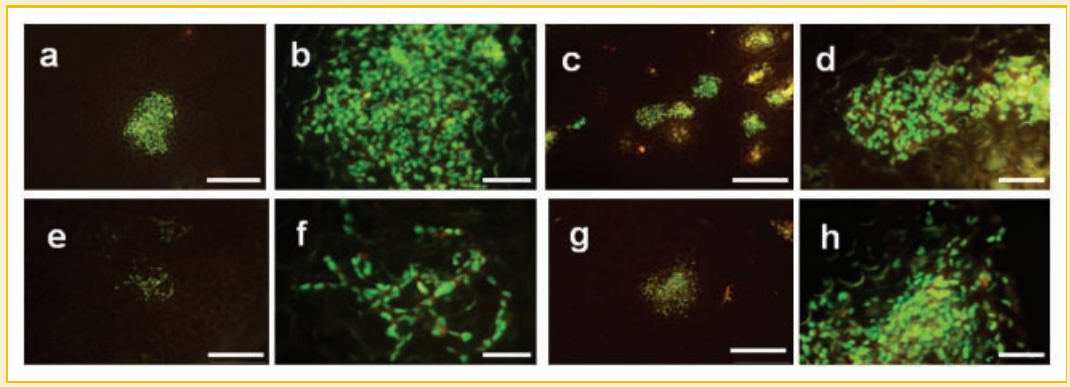

Fig. 4. Imaging of cancer cell lung colony morphology. Cancer colonies on the lung in live mice were observed 10 days after 1×10^6 dual-color HT1080 or 2×10^5 dual-color MMT cells injection. a–d: Lung metastatic colonies of dual-color HT1080. (b) is high magnification image of (a). (d) is a high-magnification image of (c). The cancer cell colonies were mostly round or oval and the margin of the colony is distinct. e–h: Lung colonies of dual-color MMT cells. (f) is a high magnification image of (e). (h) is a high-magnification image of (g). The margin of the MMT colonies is unclear and the cytoplasm of MMT cells is stretched. a,c,e,g: Scale bar, 500 μm. b,d,f,h: Scale bar, 100 μm.

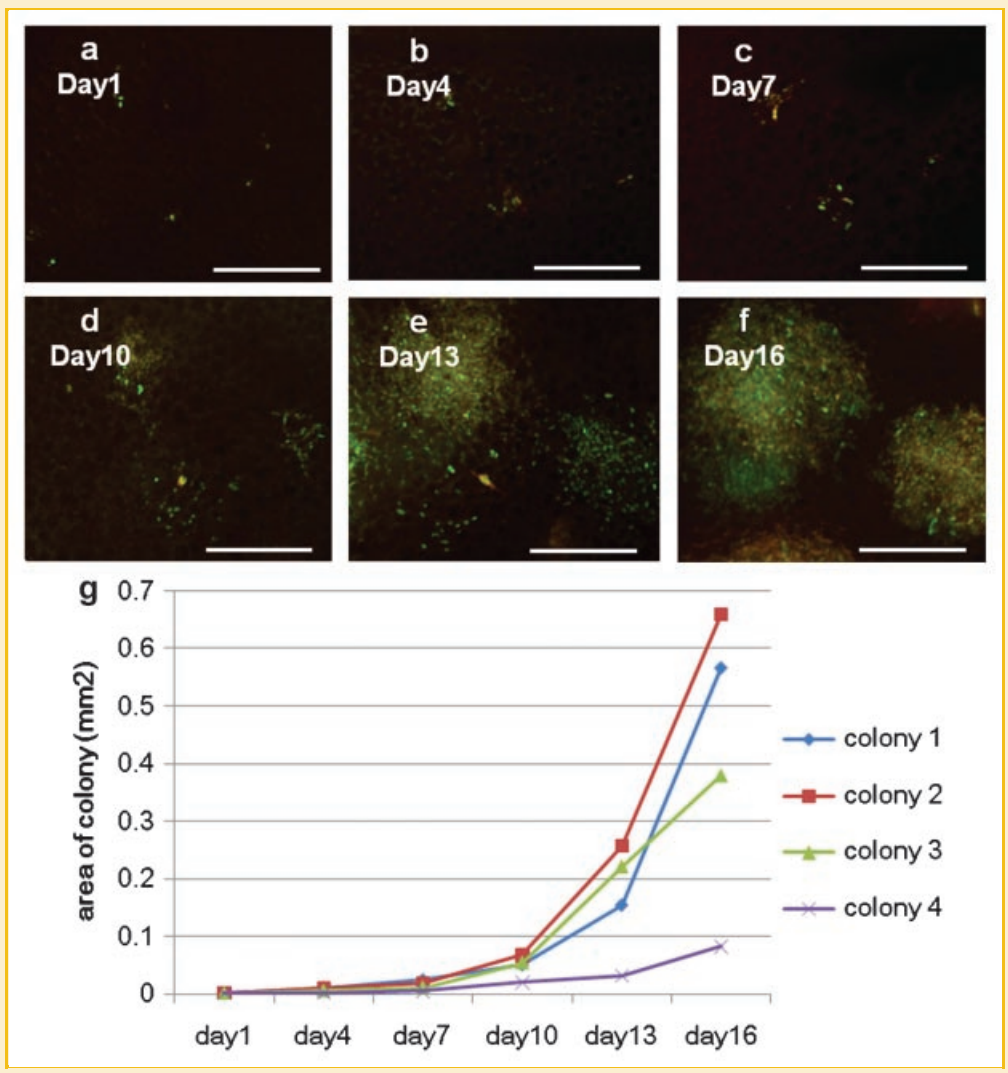

Fig. 5. Time-course imaging of cancer cell colony formation on the lung in live mice. a–f: 2×10^5 dual-color MMT cells were injected into the tail vein of nude mice at day 0. Individual colonies were followed six times from day 1 to day 16 at the same magnification. In the first week, colony growth was relatively slow, but by day 10, colonies proliferated more rapidly. Scale bar, 500 μm. g: Colony proliferation rates of dual-color MMT cells in the lung. The fluorescent area of colonies increased in an exponential fashion that was similar to their in vitro growth rate.

was relatively slow. After day 10, the growth rate rapidly increased. When these data were graphed, the growth curve was similar to that in vitro and increased exponentially (Fig. 5g).

Using this imaging technology, we could visualize the differential growth of the colonies in different parts of the lung. It appears that not all colonies have equal growth rates.

DISCUSSION

Airway access is essential for a number of experimental animal models, including observation of lung cancer or metastases, administration of substances into the lung, and pulmonary-function measurements. Intubation of mice and controlling their ventilation is important for longitudinal and repeated studies. Tracheostomy or direct tracheal puncture is easier and faster than endotracheal intubation. However, these procedures are inadequate for longitudinal and repeated studies, because it often causes air-leakage after removal of the intubation cannula. There have been some reports in the literature regarding the intubation and ventilation of mice, but these methods requires special instruments, such as a fiber-optic laryngoscope [Costa et al., 1986], small arthroscope, and videocamera system [Vergari et al., 2003], or a custom-made stage for perpendicular positioning of the mouse [Brown et al., 1999; Hamacher et al., 2008]. Our procedure, on the other hand, does not need any special instruments or perpendicular positioning. The success rate of our method was 100%, and the intubation time was comparable to previous reports [Vergari et al., 2003; Spoelstra et al., 2007]. Repeated intubation with this method had no effect on body weight compared to the control group. The small skin incision and abrasion of subcutaneous tissue had no significant toxicity to the mice and did not affect subsequent experimentation. The mouse intubation method we developed is feasible, accurate, relatively noninvasive, reproducible in the same mouse and does not require any special instrument.

To understand the mechanism of lung metastasis, it is ideal to assess changes over time in the same mouse, since there is considerable individual variability of cancer behavior in mice. In this report, we present a new in vivo mouse model to image single cancer cell dynamics of lung metastasis. We were able to image the mice repeatedly, which made it possible to observe the real-time seeding viability, growth and lung colony formation of the cancer cells, labeled with GFP in the nucleus and RFP in the cytoplasm. Observations have been carried out for up to 8 h and repeated up to six times per mouse thus far. This new technology makes it possible to observe real-time monitoring of cancer-cell dynamics of metastasis in the lung and to identify potential metastatic stem cells by their ability to form colonies in the lung, which our results suggest is a rare event.

ACKNOWLEDGMENTS

This study was supported in part by National Cancer Institute grant CA132971 to the University of California San Diego and AntiCancer Inc.

REFERENCES

Brown RH, Walters DM, Greenberg RS, Mitzner W. 1999. A method of endotracheal intubation and pulmonary functional assessment for repeated studies in mice. J Appl Physiol 87:2362–2365.

Chishima T, Miyagi Y, Wang X, Yamaoka H, Shimada H, Moossa AR, Hoffman RM. 1997. Cancer invasion and micrometastasis visualized in live tissue by green fluorescent protein expression. Cancer Res 57:2042–2047.

Costa DL, Lehmann JR, Harold WM, Drew RT. 1986. Transoral tracheal intubation of rodents using a fiberoptic laryngoscope. Lab Anim Sci 36:256–261.

Hamacher J, Arras M, Bootz F, Weiss M, Schramm R, Moehrlen U. 2008. Microscopic wire guide-based orotracheal mouse intubation: Description, evaluation and comparison with transillumination. Lab Anim 42:222–230.

Hoffman RM. 2005. The multiple uses of fluorescent proteins to visualize cancer in vivo. Nat Rev Cancer 5:796–806.

Spoelstra EN, Ince C, Koeman A, Emons VM, Brouwer LA, van Luyn MJ, Westerink BH, Remie R. 2007. A novel and simple method for endotracheal intubation of mice. Lab Anim 41:128–135.

Vergari A, Polito A, Musumeci M, Palazzesi S, Marano G. 2003. Video-assisted orotracheal intubation in mice. Lab Anim 37:204–206.

Yamamoto N, Yang M, Jiang P, Xu M, Tsuchiya H, Tomita K, Moossa AR, Hoffman RM. 2003a. Determination of clonality of metastasis by cell-specific color-coded fluorescent-protein imaging. Cancer Res 63:7785–7790.

Yamamoto N, Yang M, Jiang P, Tsuchiya H, Tomita K, Moossa AR, Hoffman RM. 2003b. Real-time GFP imaging of spontaneous HT1080 fibrosarcoma lung metastases. Clin Exp Metastasis 20:181–185.

Yamamoto N, Jiang P, Yang M, Xu M, Yamauchi K, Tsuchiya H, Tomita K, Wahl GM, Moossa AR, Hoffman RM. 2004. Cellular dynamics visualized in live cells in vitro and in vivo by differential dual-color nuclear-cytoplasmic fluorescent-protein expression. Cancer Res 64:4251–4256.

Yamauchi K, Yang M, Jiang P, Yamamoto N, Xu M, Amoh Y, Tsuji K, Bouvet M, Tsuchiya H, Tomita K, Moossa AR, Hoffman RM. 2005. Real-time in vivo dual-color imaging of intracapillary cancer cell and nucleus deformation and migration. Cancer Res 65:4246–4252.

Yamauchi K, Yang M, Jiang P, Xu M, Yamamoto N, Tsuchiya H, Tomita K, Moossa AR, Bouvet M, Hoffman RM. 2006. Development of real-time subcellular dynamic multicolor imaging of cancer-cell trafficking in live mice with a variable-magnification whole-mouse imaging system. Cancer Res 66:4208–4214.

Yang M, Baranov E, Jiang P, Sun FX, Li XM, Li L, Hasegawa S, Bouvet M, Al-Tuwaijri M, Chishima T, Shimada H, Moossa AR, Penman S, Hoffman RM. 2000. Whole-body optical imaging of green fluorescent protein-expressing tumors and metastases. Proc Natl Acad Sci USA 97:1206–1211.